Contribution of a buried aspartate residue towards the catalytic efficiency and structural stability of *Bacillus stearothermophilus* lactate dehydrogenase

Timothy J. NOBBS,* Antonio CORTÉS,† Josep Lluis GELPI,† J. John HOLBROOK,‡ Tony ATKINSON,* Michael D. SCAWEN*§ and David J. NICHOLLS*

*Division of Biotechnology, Centre for Applied Microbiology and Research, Porton, Salisbury, U.K., †Departmento Bioquimica i Fisiologia, Universitat de Barcelona, Marti i Franquès 1, Barcelona, Spain and ‡Molecular Recognition Centre, School of Medical Sciences, University Walk, Bristol, U.K.

The X-ray structure of lactate dehydrogenase (LDH) shows the side-chain carboxylate group of Asp-143 to be buried in the hydrophobic interior of the enzyme, where it makes hydrogen-bonding interactions with both the side-chain hydroxyl group of Ser-273 and the main-chain amide group of His-195. This is an unusual environment for a carboxylate side-chain as hydrogen bonding normally occurs with water molecules at the surface of the protein. A charged hydrogen-bonding interaction in the interior of a protein would be expected to be much stronger than a similar interaction on the solvent-exposed exterior. In this respect the side-chain carboxylate group of Asp-143 appears to be important for maintaining tertiary structure by providing a common linkage point between three discontinuous elements of the secondary structure, α1F, βK and the β-turn joining βG and βH. The contribution of the Asp-143 side-chain to the structure and function of *Bacillus stearothermophilus* LDH was assessed by creating a mutant enzyme containing Asn-143. The decreased thermal stability of both unactivated and fructose-1,6-diphosphate (Fru-1,6-P_2)-activated forms of the mutant enzyme support a structural role for Asp-143. Furthermore, the difference in stability of the wild-type and mutant enzymes in guanidinium chloride suggested that the carboxylate group of Asp-143 contributes at least 22 kJ/mol to the conformational stability of the wild-type enzyme. However, there was no alteration in the amount of accessible tryptophan fluorescence in the mutant enzyme, indicating that the mutation caused a structural weakness rather than a gross conformational change. Comparison of the wild-type and mutant enzyme steady-state parameters for various 2-keto acid substrates showed the mutation to have a general effect on catalysis, with an average difference in binding energy of 11 kJ/mol for the transition-state complexes. The different effects of pH and Fru-1,6-P_2 on the wild-type and mutant enzymes also confirmed a perturbation of the catalytic centre in the mutant enzyme. As the side-chain of Asp-143 is not sufficiently close to the active site to be directly involved in catalysis or substrate binding it is proposed that the effects on catalysis shown by the mutant enzyme are induced either by a structural change or by charge imbalance at the active site. As Asp-143, His-195 and Ser-273 are absolutely conserved in all known LDH sequences this charged interaction is an important and general feature of the structure/function relationship in LDH.

INTRODUCTION

The three-dimensional structure of a protein is maintained by a delicate balance of intramolecular forces consisting of several types of, usually non-covalent, interactions. Hydrogen bonding is one of the most important interactions in proteins, stabilizing both secondary structure (e.g. α-helices and β-sheets) and tertiary structure. We have assessed the contribution of a conserved hydrogen-bonding interaction to the structural and catalytic properties of *Bacillus stearothermophilus* lactate dehydrogenase (BSLDH). The X-ray structure of BSLDH shows the side-chain of Asp-143 to be hydrogen bonded, with both the hydroxyl group of Ser-273 and the main-chain amide of His-195 (Wigley et al., 1992). This type of hydrogen-bonding interaction is unusual, as this acidic amino acid side-chain is buried in the hydrophobic interior of the protein whereas most acidic side-chains are found exposed to the solvent. The amino acid residues Asp-143, Ser-273 and His-195 are absolutely conserved in all known lactate dehydrogenase (LDH) amino acid sequences, suggesting that an interaction between these residues is of general importance to the structure/function of LDHs. In the structurally and catalytically analogous enzyme malate dehydrogenase (MDH), the amino acid residue at position 143 is conserved as Asn with no residue conservation at position 273. This is a point of interest because LDH and MDH share considerable secondary and tertiary structural identity and have many functionally important amino acid residues in common (Birktoft et al., 1982; Birktoft and Banaszak, 1984). Both enzymes follow the same compulsory order binding mechanism and catalyse a similar reaction; the interconversion of a 2-keto acid and a 2-hydroxy acid using NADH/NAD^+ as a cofactor (Birktoft and Banaszak, 1984). The main functional difference between these two enzymes resides in substrate specificity.

The aim of this study was to assess the contribution of the buried side-chain of Asp-143 to the structure and function of BSLDH. Site-directed mutagenesis of the BSLDH gene was used to replace Asp-143 with Asn. In view of the conservation of Asn-143 in MDH this was the preferred choice for replacement in

Abbreviations used: LDH, lactate dehydrogenase; BSLDH; *Bacillus stearothermophilus* LDH; MDH, malate dehydrogenase; GdmCl, guanidinium chloride; Fru-1,6-P_2, fructose-1,6-diphosphate; $(K_Q)_{eff.}$, effective quenching constant; $(f_a)_{eff.}$, effective fractional maximum fluorescence; k_3, bimolecular collisional rate constant.

§ To whom correspondence should be addressed.

BSLDH in order to minimize steric disruption of structure, to maintain hydrogen-bonding potential and to characterize the effect on substrate specificity with reference to MDH.

EXPERIMENTAL

Bacterial strains and vectors

The host strain used for all recombinant plasmids and phage was *Escherichia coli* TG-1 [*lacIP*^{q} δM15-*pro*), *supE*, *thi*, *hsdD5*/*F'*,*traD36*, *proA*$^+$*B*$^+$] which was grown in YT medium (2% tryptone, 2% yeast extract, 1% NaCl) at 37 °C in the presence or absence of 100 μg/ml ampicillin. Wild-type BSLDH was produced from an *E. coli* clone containing the recombinant plasmid pLDH41 as described by Barstow et al. (1986). The mutant enzyme was produced using the same expression system, which contained a mutated *ldh* gene.

DNA-manipulation and site-directed mutagenesis

Recombinant DNA techniques were performed as described by Sambrook et al. (1989). Nucleotide sequences were determined using 'Sequenase Version 2.0' with deoxy-7-deazaguanosine, according to manufacturer's specifications (Cambridge Bioscience, Cambridge, U.K.). The mutagenic oligonucleotide (5'-TAAAATGTTGACCGGAT-3') was synthesized using an Applied Biosystems 380A DNA synthesizer. Site-directed mutations were introduced into the BSLDH gene contained in bacteriophage M13mp8 using the primer-extension method (Winter et al., 1982). The entire nucleotide sequence of the mutated gene was determined to check for the absence of unwanted secondary mutations. The mutated BSLDH gene was excised from double-stranded phage DNA as a 1.1 kb *Eco*RI/*Pst*I fragment and ligated into the *Eco*RI/*Pst*I sites of the plasmid vector pKK223-3 for expression of the gene product.

Protein purification

Wild-type and mutant BSLDHs were produced in *E. coli* as 15–25% of the soluble cell protein. Cell extracts of *E. coli* containing the cloned genes were heated at 60 °C for 30 min followed by Cibacron Blue F3GA affinity chromatography and an ion-exchange step as described previously (Hart et al., 1987).

Enzyme and protein assays

Steady-state assays were performed in 100 mM triethanolamine buffer, pH 6.0, containing various amounts of substrate and co-enzyme. Rates were determined by measuring the change in NADH absorbance at 340 nm. When steady-state constants were determined in the presence of fructose-1,6-diphosphate (Fru-1,6-P_2) enzyme solutions were preincubated in Fru-1,6-P_2 for 20 min at 4 °C before assay. Steady-state assays were determined at different pH values in 100 mM triethanolamine buffer containing 100 mM NaCl adjusted to the required pH with 250 mM NaOH/100 mM NaCl to maintain a constant ionic strength. Steady-state kinetics were performed with 0.2 mM NADH and various concentrations of pyruvate in the presence of Fru-1,6-P_2. The Fru-1,6-P_2 concentration was 5 mM for measurements in the pH range 6.0–8.0 and increased to 20 mM for determinations in the pH range 8.0–9.0 to maintain saturation of the allosteric site. Protein concentrations of purified BSLDH preparations were determined by measuring the absorbance at 280 nm ($E^{1\%}_{280}$ 8.5).

Equilibrium unfolding in guanidinium chloride (GdmCl)

Enzyme preparations (0.3 μM subunits) were equilibrated in 20 mM phosphate buffer, pH 7.4, containing 1 mM dithiothreitol and various concentrations of GdmCl for 16 h at 25 °C. Solutions were excited at 295 nm and the change in tryptophan fluorescence emission monitored at 345 nm using a Perkin–Elmer LS5 fluorescence spectrophotometer. ΔG^{H_2O} for each transitional change was calculated using the method described by Pace et al. (1989) and fitting the observed data by non-linear regression as described below.

The first, second and third transitions in the GdmCl-unfolding curve are described by *Tn*, *Tn2*, and *Tn3* respectively:

$$Tn1 = \exp\{[(m1 \cdot G) - E1]/RT\}$$

$$Tn2 = \exp\{[(m2 \cdot G) - E2]/RT\}$$

$$Tn3 = \exp\{[(m3 \cdot G) - E3]/RT\}$$

where: G is the GdmCl concentration (M); R, the gas constant (kJ/mol per K); T, the temperature (K); $m1$, $m2$ and $m3$, the gradients of the first, second and third transitions respectively; $E1$, $E2$ and $E3$, the $\Delta G^{(H_2O)}$ for the first, second and third transitions respectively. Each transition, $Tn(1, 2$ and $3)$ is considered as a ratio of the forms of the protein undergoing the transition. This is expressed as a fraction by the terms $Tnx/(1 + Tnx)$ (where $x = 1, 2$ and 3) and is related to the change in fluorescence of each respective transition by the term dFx. The equations for Tnx define ΔG for each transition as the y-axis intercept of a linear transform of the data as described by Pace et al. (1989). The curve was fitted to the data points by solving for Y in eqn (1) using the curve-fitting facility of Sigmaplot version 4.1 (Jandel Scientific).

$$Y = F0 + dF1 \cdot Tn1/(1 + Tn1) + dF2 \cdot Tn2/(1 + Tn2) + dF3 \cdot Tn3/(1 + Tn3) \quad (1)$$

where: Fo is initial fluorescence, d$F1$ the change in fluorescence of the first transition, d$F2$ the change in fluorescence of the second transition, and d$F3$ the change in fluorescence of the third transition.

Fluorescence quenching

The change in fluorescence emission of enzyme solutions (8 μM subunits) at 345 nm was measured with excitation at 295 nm in various amounts of KI (quencher). Solutions were made from a stock of 5 M KI containing 0.1 mM sodium thiosulphate in 20 mM phosphate buffer, pH 7.4.

Determination of protein thermal stability

Irreversible enzyme inactivation was measured. Enzyme solutions were diluted into 100 mM triethanolamine buffer (adjusted to pH 6.0 at the working temperature) to a concentration of 20 μg/ml and Fru-1,6-P_2 was added to a final concentration of 5 mM when appropriate. Aliquots (50 μl) in microfuge tubes were sequentially placed in a water bath incubated at the appropriate temperature for a time course of up to 1 h. At the end of the incubation period all the tubes were simultaneously removed and placed on ice for a relaxation time of 10 min before assay for residual enzyme activity. Unheated enzyme solution was used as the zero time control.

Electrophoresis

Proteins were analysed by SDS/PAGE and isoelectric-focusing gel electrophoresis using the Phastgel system (Pharmacia, Milton Keynes, Bucks., U.K.).

Theoretical calculations

Models of BSLDH structures at different steps of the catalytic pathway, available from earlier work (Gelpi et al., 1993), were used to build the corresponding mutant structures. The side-chain of Asp-143 was changed to Asn using the molecular modelling package INSIGHT II (Biosym Technologies, Basingstoke, Hants., U.K.) and the new side-chain relaxed in the different structures using a few iterations of steepest descents. The structures were further minimized using conjugate gradients until a maximum derivative of less than 0.004 kJ/mol was achieved. The relative permittivity was fixed to 2 and a sphere of explicit water molecules within 1.5 nm (15 Å) of the new side-chain was included in order to mimic solvent screening, only residues in close contact with the side-chain were allowed to move. Molecular mechanics were performed using DISCOVER 2.9 implemented in an Alliant FX-80 computer. The all-atom consistent valence force-field parameters and charges were used (Dauber-Osguthorpe et al., 1988). Electrostatic-interactions energies were determined as described elsewhere (Gelpi et al., 1993). Electrostatic potentials were calculated using the Poisson–Boltzmann equation, solved by the finite difference method, as implemented in the program DELPHI (Gilson et al., 1987) (Biosym Technologies). All calculations were carried out with the assigned relative permittivities of 2 inside the protein and 80 for bulk water at an ionic strength of 0.145 M. Energies were deduced from the calculated potentials and a set of electrostatic point charges for the amino acid residues.

RESULTS

The role of Asp-143 in wild-type BSLDH was investigated by substituting it with Asn to remove the acidic amino acid side-chain while conserving size, shape and polarity. The X-ray structure of BSLDH (Wigley et al., 1992) indicates potential hydrogen-bonding interactions between the side-chain of Asp-143, the side-chain of Ser-273 and the main-chain amide group of His-195 (Figure 1). These interactions are buried in the interior of the protein and together provide a link between three elements of secondary structure; α-1F, β-K and the β-turn βG-βH (Figure 1). As all these amino acid residues are absolutely conserved among LDHs it is likely that the Ser-273–Asp-143 His-195 amide interaction is a common feature of the LDH framework.

Steady-state catalysis and Fru-1,6-P_2 activation

The mutation, Asp-143→Asn was found to have an adverse effect on the K_m and $k_{cat.}$ values for pyruvate and various other

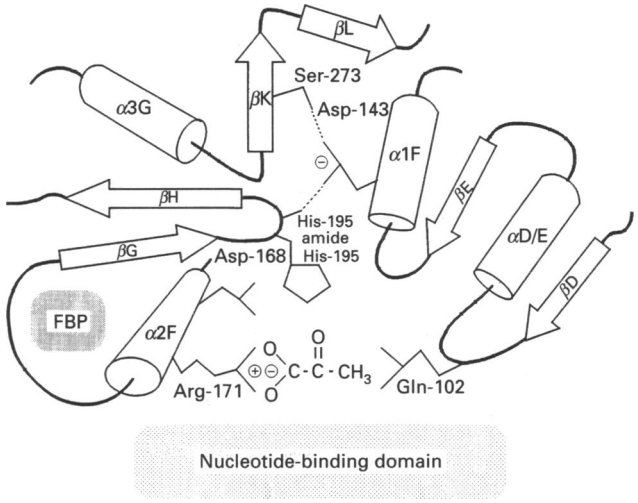

Figure 1 Diagram of BSLDH showing the region of Asp-143 in relation to the active-site and some elements of secondary structure

Arrow, β-sheet (arrow head denotes C-terminus of sheet); cylinder, α-helix; bold line, connecting structure; amino acid residue side-chains are indicated by numbers; shaded area denoted FBP, location of Fru-1,6-P_2-binding site; some relevant charged groups are circled; broken lines, potential hydrogen bonds.

Table 1 Steady-state kinetic constants for the wild-type and mutant enzymes

Initial velocities were determined at 25 °C in 100 mM triethanolamine buffer, pH 6.0. When required 5 mM Fru-1,6-P_2 was included in the assay mixture and enzymes were preincubated in 5 mM Fru-1,6-P_2 for 30 min before assay. Kinetic constants for pyruvate were determined in 0.2 mM NADH for all 2-keto acid substrates. Kinetic constants for NADH with Fru-1,6-P_2 were determined in 2 mM for the wild-type enzyme and 50 mM for the mutant enzyme.

Substrate measured	+/− Fru-1,6-P_2	Steady-state constant	Enzyme: Wild type (Asp-143)	Enzyme: Mutant (Asn-143)
Pyruvate	−	K_m (mM)	4.5	25
		$k_{cat.}$ (s^{-1})	190	24
		$k_{cat.}/K_m$ ($M^{-1} \cdot s^{-1}$)	42000	960
Pyruvate	+	K_m (mM)	0.08	3.6
		$k_{cat.}$ (s^{-1})	178	61
		$k_{cat.}/K_m$ ($M^{-1} \cdot s^{-1}$)	2200000	17000
2-Oxobutyrate	+	K_m (mM)	0.68	1.23
		$k_{cat.}$ (s^{-1}	187	7
		$k_{cat.}/K_m$ ($M^{-1} \cdot s^{-1}$)	280000	5600
2-Oxovalerate	+	K_m (mM)	4.3	4.7
		$k_{cat.}$ (s^{-1}	51	1.2
		$k_{cat.}/K_m$ ($M^{-1} \cdot s^{-1}$)	12000	250
Oxaloacetate	+	K_m (mM)	1.6	6.3
		$k_{cat.}$ (s^{-1})	10	0.14
		$k_{cat.}/K_m$ ($M^{-1} \cdot s^{-1}$)	3800	22
NADH	+	K_m (mM)	0.03	0.03

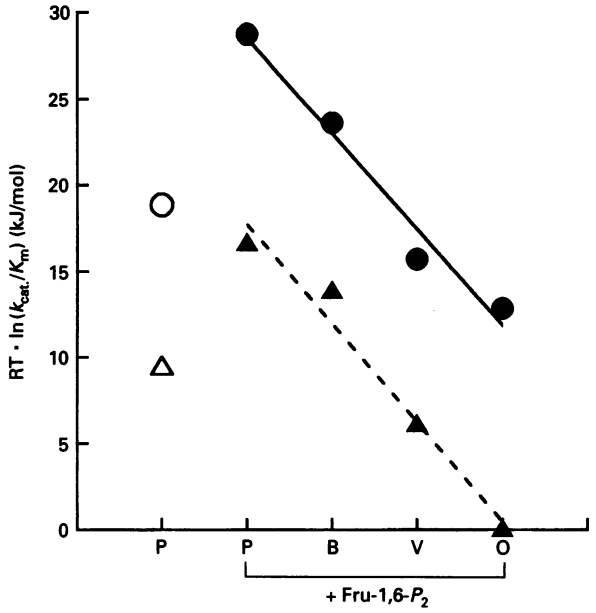

Figure 2 Binding energies for the transition-state complex of various 2-keto acid substrates

Binding energies relative to the mutant enzyme with oxaloacetate were calculated using the equation: $\Delta G = \boldsymbol{R}T \cdot \ln[(k_{cat.}/K_m)_A/(k_{cat.}/K_m)_B]$ where $\boldsymbol{R}$ is the gas constant (kJ/mol per K), T is temperature (K); $(k_{cat.}/K_m)_A$, various for enzymes and substrates and $(k_{cat.}/K_m)_B$, mutant enzyme with oxaloacetate. ○, Wild-type enzyme without Fru-1,6-P_2; △, mutant enzyme without Fru-1,6-P_2; ●, wild-type enzyme with 5 mM Fru-1,6-P_2; ▲, mutant enzyme with 5 mM Fru-1,6-P_2. Substrate abbreviations: P, pyruvate; B, 2-oxobutyrate; V, 2-oxovalerate; O, oxaloacetate.

2-keto acid substrates (Table 1). However, there was no significant change in the K_m value for NADH, indicating that the effects of the mutation on catalysis were confined to the substrate-binding site. The term $k_{cat.}/K_m$ can be used to calculate the binding energy of the transition-state complex by using the equation $\boldsymbol{R}T \cdot \ln(k_{cat.}/K_m)$ (Wilkinson et al., 1983). Analysis of the mutant enzyme by a method which considers only the transition state has the advantage of excluding any secondary effects of the mutation on other processes (such as non-productive binding, induced fit, etc.) which do not result in a catalytically competent transition-state complex (Fersht et al., 1985). To interpret the effect of Asp-143 it is important to consider only the relative binding energies for the transition-state complexes of various 2-keto acid substrates with the wild-type and mutant enzymes. For this reason the binding energies presented in Figure 2 are relative to the lowest productively bound complex measured in this study, that of oxaloacetate with the mutant enzyme. The mutant enzyme showed the same general trends as the wild-type enzyme, with no relative enhancement in specificity for any of the substrates used. When activated by Fru-1,6-P_2, the average difference in relative binding energy between the wild-type and mutant enzymes, for all four 2-keto acid substrates was about 11 kJ/mol. This was similar to the difference in relative binding energy for pyruvate (10 kJ/mol) to the unactivated forms of each enzyme (Figure 2). This shows that the mutation has produced a decrease in the relative binding energies for all the transition-state complexes in a way which appears to be independent of Fru-1,6-P_2 activation or the type of 2-keto acid substrate.

Allosteric activation of BSLDH by the effector Fru-1,6-P_2 involves a change in quaternary structure, from a dimer

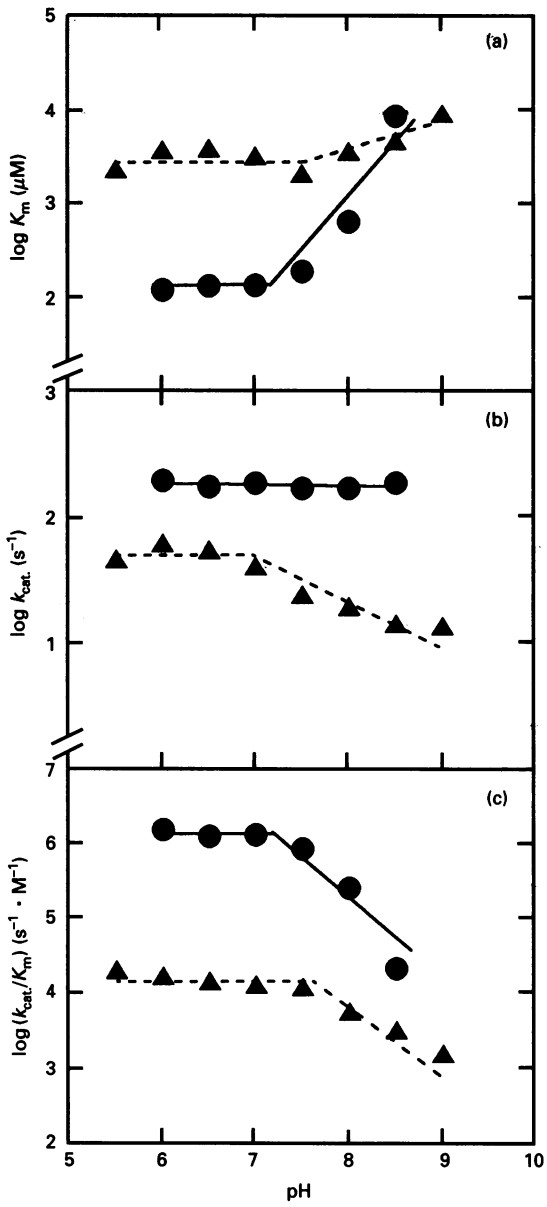

Figure 3 Steady-state kinetic parameters determined at different values of pH

Steady-state constants were determined in two overlapping buffer systems, 100 mM L-histidine (pH 5.5–7.0) and 100 mM triethanolamine (pH 6.5–8.5). Each buffer was 20 mM containing 100 mM NaCl and adjusted to the desired pH with 100 mM NaOH (or HCl) containing 100 mM NaCl to ensure constant ionic strength. (**a**), log(K_m) (μM) versus pH; (**b**), log($k_{cat.}$) (s^{-1}) versus pH; (**c**), log($k_{cat.}/K_m$) ($s^{-1} \cdot M^{-1}$) versus pH; symbols are: ●, wild-type enzyme, and ▲, mutant enzyme.

(unactivated form) to a tetramer (Fru-1,6-P_2-activated form), which enhances both thermal stability and catalytic efficiency (Clarke et al., 1985). The amount of enzyme in the Fru-1,6-P_2-activated form can be estimated by measuring the relative rate enhancement at low concentrations of pyruvate for enzyme solutions equilibrated in different concentrations of Fru-1,6-P_2. The activation constant (K_a) was determined for both the wild-type and mutant enzymes as the concentration of Fru-1,6-P_2 required for half-maximum rate enhancement. The value of K_a is a measure of the overall activation effect and contains components relating to both Fru-1,6-P_2-binding affinity and the

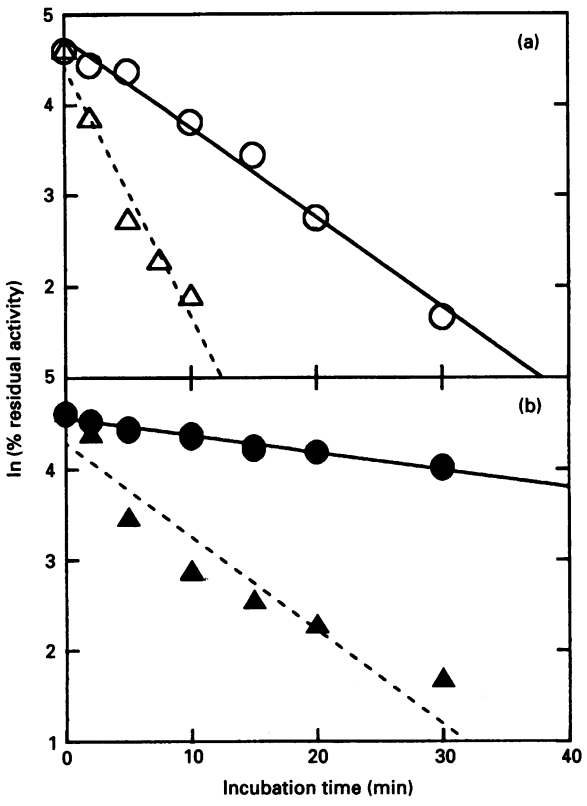

Figure 4 Irreversible thermal inactivation of wild-type and mutant enzymes

(**a**) Inactivation at 75 °C, without Fru-1,6-P_2, (○) wild-type enzyme $t_{\frac{1}{2}}$ = 7 min, (△) mutant enzyme $t_{\frac{1}{2}}$ = *2.5 min.* (**b**) Inactivation at 80 °C, in 5 mM Fru-1,6-P_2, (●) wild-type enzyme $t_{\frac{1}{2}}$ = 37 min, (▲) mutant enzyme $t_{\frac{1}{2}}$ = 7 min.

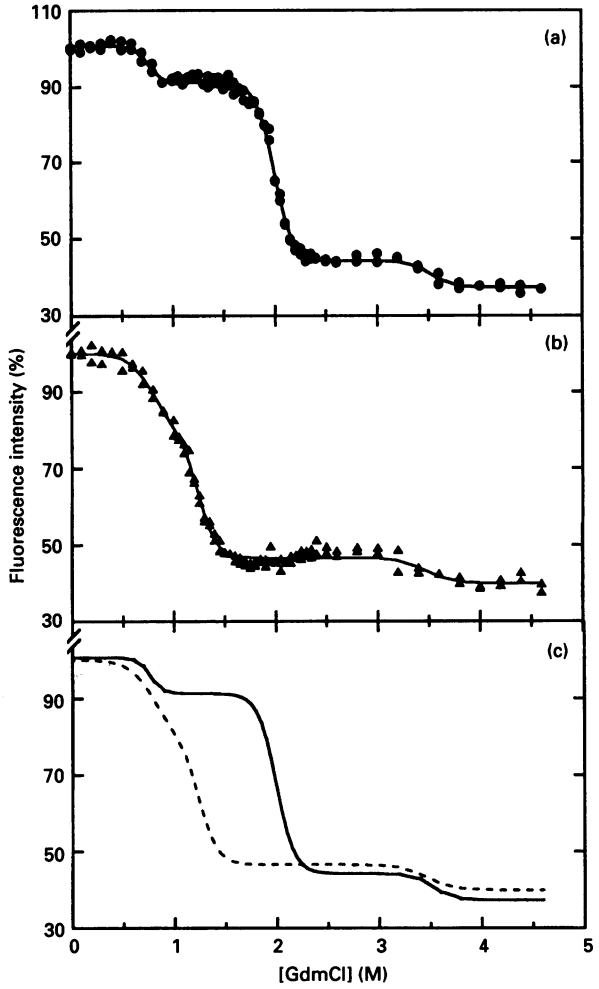

Figure 5 Equilibrium unfolding profiles in GdmCl

To facilitate comparison the data are presented as percentages of initial fluorescence emission intensity in the absence of GdmCl for wild-type enzyme (**a**), and mutant enzyme (**b**). Unfolding profiles for the wild-type (——) and mutant (– – –) enzymes (**c**) were calculated by non-linear regression analysis. The initial fluorescence emission intensity of the mutant enzyme was 15% of the wild type (see text for experimental details).

structural rearrangements which occur upon allosteric activation, but is not a dissociation constant for Fru-1,6-P_2. K_a was found to be 0.09 mM for the wild-type and 0.27 mM for the mutant enzymes. As K_a is an equilibrium constant the difference in energy between the wild-type and mutant enzymes ($\Delta\Delta G^t$) for catalytic activation by Fru-1,6-P_2 can be expressed as $RT \cdot \ln[K_a(\text{wild type})/K_a(\text{mutant})]$. The mutant enzyme was over 95% activated at 5 mM Fru-1,6-P_2, indicating that the physiochemical and catalytic properties measured in subsequent experiments at 5 mM Fru-1,6-P_2 were not due to undersaturation by Fru-1,6-P_2. With the preferred substrate, pyruvate, Fru-1,6-P_2 activation of the wild-type enzyme was governed by a decrease in K_m but with little effect on $k_{cat.}$ (Table 1). In the case of the mutant enzyme, Fru-1,6-P_2 activation affects both K_m and $k_{cat.}$ for pyruvate. The effect of Fru-1,6-P_2 on both $k_{cat.}$ and K_m has been observed in other mutants of BSLDH, which was explained by the substrate binding non-productively to the mutant enzyme (Hart et al., 1987).

Effect of pH

Productive substrate binding is linked to the ionization state of LDH such that pyruvate can only bind when the essential His-195 residue is protonated (Holbrook and Stinson, 1973). The ionization state of His-195 in the binary complex (enzyme–NADH) can therefore be monitored by measuring $k_{cat.}/K_m$ for pyruvate as a function of pH. Plots of log $k_{cat.}/K_m$ (pyruvate) versus pH can be subdivided into two linear portions where the intercept is the apparent pK_a of His-195 in the binary complex (Figure 3c). This is about pH 7.0 and pH 7.5 for the wild-type and mutant enzymes respectively. For the mutant enzyme, the change in K_m over the pH range 7.0–9.0 was much less than the change in K_m for the wild-type enzyme in the same region (Figure 3a). For the wild-type enzyme $k_{cat.}$ remained constant over the pH range 7.0–9.0 but decreased markedly for the mutant enzyme (Figure 3b). The different pH profiles were not due to pH inactivation of either enzyme, as full activity was retained after incubation for 1 h in pH 9 buffer. The net effect of the mutation was to introduce a pH-dependent decrease in both $k_{cat.}$ and K_m for pyruvate when compared with the wild type enzyme.

Effect of temperature

Irreversible enzyme inactivation was used to measure protein thermal stability in the presence and absence of 5 mM Fru-1,6-P_2 (Figure 4). In the absence of Fru-1,6-P_2 and at 75 °C the wild-type enzyme had a half-life of 7 min and the mutant one of

Table 2 Non-linear regression analysis of equilibrium unfolding in GdmCl

The equation described in the text was fitted to the data presented in Figure 5 using the curve-fitting facility of Sigma Plot version 4.1 (Jandel Scientific). *E1–E3*, $\Delta G^{(H_2O)}$ for the first, second and third transitions respectively; mid 1–3, mid-point GdmCl concentration for unfolding of the first, second and third transitions respectively. The difference in $\Delta G^{(G_2O)}$ for the first and third transitions are not given due to the large error involved in calculating these values.

	$\Delta G^{(H_2O)}$ (kJ·mol^{-1})			GdmCl transition mid-point		
Enzyme	E_1	E_2	E_3	Tn_1	Tn_2	Tn_3
Wild type (Asp-143)	33±10	56±2	94±47	0.76	2.00	3.53
Mutant (Asn-143)	16±4	34±5	67±36	0.78	1.24	3.46
Difference	–	22	–	0.02	0.76	0.07

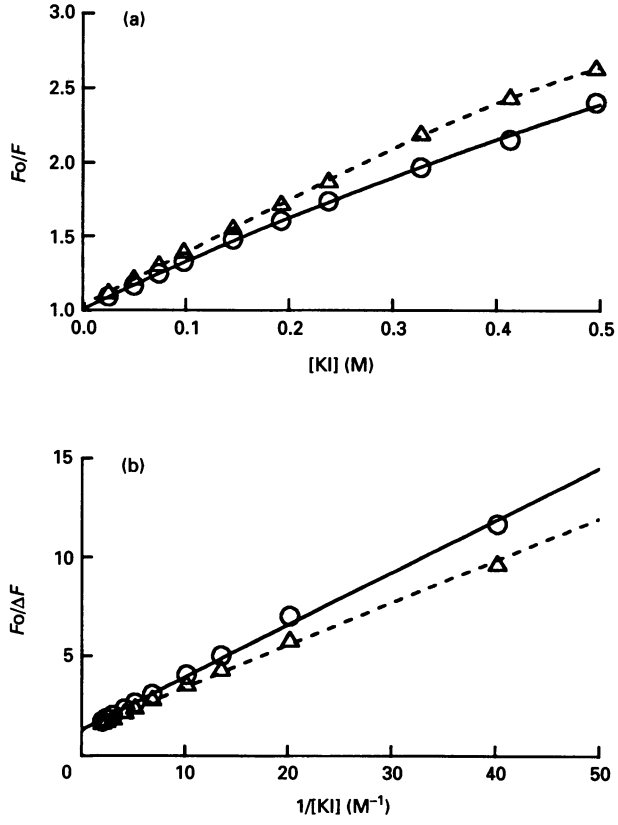

Figure 6 Iodide fluorescence quenching of the wild-type and mutant enzymes

(**a**) Stern–Volmer plot shows a non-linear relationship for both enzymes. (**b**) Modified Stern–Volmer plot shows a linear relationship for both enzymes where $1/(f_a)_{eff.}$ = intercept and $1/(f_a)_{eff.} \cdot 1/(K_Q)_{eff.}$ = slope (see text for details). (○), Wild-type enzyme; (△), mutant enzyme.

2.5 min. In the presence of Fru-1,6-P_2 and at 80 °C the wild-type enzyme had a half-life of 37 min and the mutant 7 min. This clearly shows that the mutant enzyme was less thermostable than the wild-type enzyme in both the presence and absence of Fru-1,6-P_2, although addition of Fru-1,6-P_2 did enhance the stability of the mutant enzyme.

Analysis of structure

When excited at 295 nm the fluorescence emission of the mutant enzyme at 345 nm was only about 15% lower than that of the wild-type enzyme, suggesting that the mutation had relatively little effect on gross structure and the environments of the three tryptophan fluorophores. This was not unexpected as Trp-80, Trp-150 and Trp-203 are over 2.8 nm (28 Å), 1.2 nm (12 Å) and 1.8 nm (18 Å) respectively from the carboxylate group of Asp-143.

Unfolding of BSLDH in GdmCl can be correlated with increased solvation of the tryptophan fluorophores; which is monitored by following the concomitant decrease in tryptophan fluorescence intensity. The equilibrium unfolding of wild-type BSLDH in GdmCl has a unique profile which is characterized by three transitions in the ranges 0.5–1.0 M, 1.5–2.3 M and 3–4 M GdmCl (Figure 5a). The nature of each transition has been characterized previously by Smith et al. (1991); the first transition represents primarily loss of quaternary structure from dimer to monomer, the second transition represents loss of tertiary structure, and the third transition represents unfolding of secondary structure to yield the fully denatured enzyme. The equilibrium unfolding constants determined by non-linear regression analysis are presented in Table 2. The substantial overlap between the first and second transitions (Figure 5) illustrates the benefit of using non-linear regression to interpret multiple transitions which are either well separated (wild-type) or poorly separated (mutant). It would otherwise be impossible to characterize these transitions by replotting the data as a conventional linear transformation. No assumptions were made regarding the identity of the transitions before the curve-fitting procedure. The values for the fitted parameters were used to calculate the mid-point of unfolding for each transition (Table 2). As the mid-points (calculated after curve-fitting) of the first and third transitions were found to be very similar for both wild-type and mutant enzymes and these transitions were approx. superimposable (Figure 5c), they were assumed to be identical. The errors involved in determining $\Delta G^{(H_2O)}$ for the first and third transitions were high due to the relatively small change in fluorescence intensity in these regions, for this reason the differences are not given in Table 2. The effect of the mutation was primarily on the comparatively well-defined second transition, i.e. tertiary structure, such that the folded conformation of the mutant enzyme was destabilized by about 22 kJ/mol (subunits).

Iodide fluorescence quenching

The accessibility of the fluorophores in the wild-type and mutant enzymes was investigated by using iodide ions to quench the excited fluorophores by radiationless collisional deactivation (Figure 6). Both the wild-type and mutant enzymes were typical of proteins containing several tryptophan side-chains in different environments, and produce the characteristic curved Stern–Volmer plot (Figure 6a). The modified Stern–Volmer plot of $F_o/\Delta F$ versus 1/[KI] (Figure 6b) was used to quantify the difference between the wild-type and mutant enzymes in terms of the effective quenching constant, $(K_Q)_{eff.}$ = intercept/slope, and the effective fractional maximum fluorescence, $(f_a)_{eff.}$ = 1/intercept (Lehrer, 1971):

$$F_o/\Delta F = \left[\frac{1}{[KI]} \cdot \frac{1}{(f_a)_{eff.}} \cdot \frac{1}{(K_Q)_{eff.}}\right] + \frac{1}{(f_a)_{eff.}} \quad (2)$$

For the wild-type and mutant enzymes $(f_a)_{eff.}$ were identical (0.77), indicating that 77% of tryptophyl fluorescence was

accessible to quenching in both enzymes. This suggests that the mutation did not cause a gross disturbance of the protein structure, although this method is not sufficiently sensitive to identify any subtle changes which may have occurred in the fine structure of the mutant enzyme.

As Asp-143 is screened from the bulk solvent, general assumptions about the ionization state of the carboxyl side-chain of Asp-143 do not necessarily hold. It was therefore important to determine the ionization state of the carboxyl side-chain of Asp-143 in the wild-type enzyme. Due to uncertainties in the dielectric nature of the local environment of Asp-143 the problem was addressed on the basis that an ionized, and negatively charged, side-chain of Asp-143 would alter the overall net charge of the wild-type enzyme when compared with the neutral Asn-143 side-chain of the mutant enzyme. In this respect there was a notable difference in the value of $(K_Q)_{eff.}$; 4.9 M^{-1} for the wild-type and 6.1 M^{-1} for the mutant enzyme (Figure 6). Lehrer (1971) demonstrated that fluorescence quenching is predominantly a collisional process as $(K_Q)_{eff.}$ is directly proportional to the bimolecular quenching rate constant, k_3. In addition, a relationship was established between k_3 and molecular charge, such that k_3 was decreased in compounds with a net negative charge. The lower value of $(K_Q)_{eff.}$ for the wild-type enzyme is consistent with a greater net negative charge when compared with the mutant. This reduces the effective quenching by decreasing the bimolecular collisional rate constant (k_3) due to charge repulsion with the negative iodide ions. In addition, the lower pI of the wild-type enzyme (pI = pH 5.33) compared with that of the mutant enzyme (pI = pH 5.6) is consistent with the wild-type enzyme being more negatively charged. These two observations strongly suggest that Asp-143 is ionized in the wild-type enzyme.

DISCUSSION

Kinetics

The difference in the transition-state binding energies between the wild-type and mutant enzymes was similar for each of the 2-keto acid substrates examined, with no effect on substrate selectivity (Figure 2). This trend was also found by Hart et al. (1987) for the mutation Arg-171→Lys, a residue which interacts directly with the C-1 carboxylate group of the substrate. The mutation Asp-143→Asn caused an average decrease in binding energies for the transition-state complexes of 11 kJ/mol. This was much less than the average decrease reported by Hart et al. (1987) of 25 kJ/mol for mutation of a residue (Arg-171→Lys) which binds directly with the substrate. This difference between the transition-state binding energies of these two mutant enzymes is not unexpected as Asp-143 is approx. 0.9 nm (9 Å) from the substrate-binding site and is therefore unlikely to affect binding in such a direct manner. It is more likely that the effects on substrate-binding energy are an indirect result of the mutation Asp-143→Asn, where the equal perturbation of the binding energy for the transition-state complex of each substrate is due to some unifying factor, e.g. a strained binding interaction with common functional group(s) of the substrate or disturbance of the charge balance in the active site.

The mutation has clearly attenuated the strict dependence of steady-state kinetic constants on pH (Figure 3). The simultaneous pH-dependent decrease in $k_{cat.}$ and K_m of the mutant enzyme can be partially explained as the result of pH-dependent non-productive binding, where non-productive enzyme·substrate complex(es) is in competition with the productive enzyme–substrate complex at high values of pH. The pH-dependent non-productive binding in the mutant enzyme is consistent with a non-productive ternary complex where the substrate binds to the unprotonated form of His-195 at high pH. This type of ternary complex is normally strictly excluded in the wild-type enzyme (Nicholls et al., 1993). This effect involves non-productive complexes, as the gradients for the changes in $k_{cat.}/K_m$ at pH values > 7 are similar in both wild-type and mutant enzymes with a slope of approx. 1 (Figure 3c), this is indicative of a single ionization event in both enzymes (Dixon and Webb, 1979).

Theoretical calculations

The perturbed pH characteristics of the mutant enzyme suggest that the charge balance of the active site has been disturbed. Theoretical analysis suggests that most results are due to the long-range electrostatic effect of the change Asp-143→Asn. Recently, Gelpi et al. (1993) have separately evaluated the electrostatic contribution to: substrate binding, co-enzyme binding, protonation of His-195, the substrate-induced conformational change and the stabilization of the transition state. This was done from the interaction electrostatic energies of all residues in the BSLDH subunit which, from the residues outside the active site, revealed Asp-143 as one of the most influential in LDH catalysis. The interaction energies in the wild-type BSLDH structures indicated that the Asp-143 net charge destabilizes both NADH, binding (4.37 kJ/mol) and pyruvate binding (10.37 kJ/mol) but favours His-195 protonation, as the interaction energy with its protonated form is −24.4 kJ/mol in the ternary loop-open structure. Finally, the contribution of Asp-143 net charge to the activation energy was favourable but negligible (−0.75 kJ/mol). These energies, however, cannot be directly applied to predict the properties of the Asp-143→Asn mutant as they include no information about possible conformational changes in the mutant structures. Thus, interaction energies were recalculated using minimized wild-type and mutant structures where differences between the Asp-143 and Asn-143 interaction energies would give a closer prediction of the mutant properties. From the experimental results only the K_m value for pyruvate has a direct theoretical counterpart. Calculations indicate that the Asp-143→Asn mutation would destabilize pyruvate binding by 25.5 kJ/mol. The change in direct interaction energy is −10 kJ/mol, hence, removal of the charged Asp side-chain would improve pyruvate binding. However, it is found that changes in the interaction energies of the active-site residues compensate for this effect and give an overall predicted increase of the K_m for pyruvate, as was found experimentally. This constitutes an example of how a precise electrostatic balance is necessary, as differences in structure are small and most of the effect comes from changes in the solvent screening of the already existing interactions. An exact match between theoretical and experimental energies would need, at least, to consider changes in the solvation energy that cannot be deduced from the present approach. Unfavourable, but smaller changes were found for L-lactate and co-enzymes, indicating that, among LDH substrates, pyruvate binding is the process with a greater electrostatic contribution. Effects on the other steps of the catalytic pathway were also calculated and showed that the influence of the mutation on the activation energy of the chemical transformation was negligible. As the rate-limiting step is a conformational change before the chemical transformation (Waldman et al., 1988), the calculations suggest that this protein rearrangement remains the limiting step in the mutant enzyme. The experimental changes in $k_{cat.}$ values would come from an

alteration of the precise balance of electrostatic and hydrophobic energies that drive loop closure (Gelpi et al., 1993).

Analysis of the predicted changes in the His-195 pK_a introduce some concern, as pK_a shifts are among the most accurate predictions of theoretical electrostatic analysis. The calculated differences in the electrostatic contribution of protein residues to His-195 protonation clearly indicated that with presently used models, the Asp-143→Asn mutation reduces His-195 pK_a by 2.8 units (apoenzyme), 3.9 units (binary LDH–NADH), and 2.7 units (ternary loop-open LDH). The three models used coincide to predict a pK_a shift opposite to the experimental value. In the case of BSLDH the analysis fails to predict the pK_a of His-195, which is in agreement with an earlier study (Gelpi et al., 1993). At this point, there is no explanation for this discrepancy. Whether it is a fault of the theoretical method used, either in the electrostatic calculation itself or in the charge distribution of the models used, or it is an indication of a more complex pH dependence is under study. However, an interesting result arises from the comparison of the protonation energies of loop-closed (there is no possible protonation of the closed structure, as His-195 is not solvent exposed, this energy refers to the difference between closed protonated and unprotonated enzymes) and loop-open enzyme, which reduce from −69.2 kJ/mol for the wild-type structure to 19.9 kJ/mol for the Asn-143 mutant. This result provides further support for they hypothesis that significant non-productive binding of pyruvate to an unprotonated enzyme can occur in the mutant.

The mutation Asn-143 had a marked effect on $k_{cat.}$ and K_m, both of which were altered upon activation of the mutant enzyme by Fru-1,6-P_2 (Table 1). A similar effect was observed by Hart et al. (1987) with a mutant enzyme which was altered at the substrate-binding site; this was explained by non-productive binding of the substrate to the mutant enzyme. The effect can be explained in this context, as a structural disturbance or charge imbalance caused by mutation of Asp-143 would compromise the geometry of the substrate-binding site and allow the proportion of substrate bound non-productively to be increased.

Analysis of structure

There was a marginal effect on allosteric activation of the mutant enzyme, showing only a small change in the Fru-1,6-P_2 activation energy ($\Delta\Delta G' = 2.7$ kJ/mol). There is substantial evidence which indicates that Fru-1,6-P_2 activation of BSLDH is closely linked to both inter- and intra-subunit structural changes (Clarke et al., 1986; Piontek et al., 1990; Wigley et al., 1992). The mechanism of Fru-1,6-P_2 activation can be represented in its simplest form by the following scheme:

$$2(\text{Dimer}) + 2(\text{Fru-1,6-}P_2) \overset{\text{Ligand association}}{\rightleftharpoons} 2(\text{Dimer:Fru-1,6-}P_2)$$

$$\overset{\text{Protein association}}{\rightleftharpoons} \text{Tetramer:(Fru-1,6-}P_2)_2$$

where the dimer has low catalytic efficiency, dimer:Fru-1,6-P_2 is partially activated and tetramer:(Fru-1,6-P_2)$_2$ is fully activated. As the site of the mutation is remote from the effector site (Figure 1), a direct effect of Asn-143 on Fru-1,6-P_2 binding is unlikely. A more plausible explanation is that the mutation has perturbed a Fru-1,6-P_2-dependent structural change which is required for catalytic activation. The altered equilibrium is also unlikely to have a direct effect on tetramer formation, as the mutation is remote from the subunit interface of the tetramer. Thus the small effect of the mutation Asp-143→Asn on Fru-1,6-P_2 activation provides supportive evidence for an intra-subunit molecular rearrangement. The interaction of Asp-143 with Ser-273 between α1F, βK and the β-turn βG-βH exerts comparatively little influence on Fru-1,6-P_2 activation in contrast with the much larger destabilizing effect observed when a hydrogen-bonding interaction between the β-turn βG-βH and αH is removed (Nicholls et al., 1993). The results for the Asp-143→Asn mutation are in agreement with X-ray structural evidence (Piontek et al., 1990) which shows that the subtle intra-subunit molecular rearrangement which occurs upon Fru-1,6-P_2 activation is remote from the region of Asp-143.

Regarding irreversible thermal inactivation of the mutant enzyme there are two effects to consider: (i) the mutant enzyme was less thermostable than the wild-type enzyme in both the presence and absence of Fru-1,6-P_2, suggesting that an interaction is lost in the mutant enzyme in both forms; (ii) the presence of Fru-1,6-P_2 was found to enhance the stability of the mutant enzyme, suggesting that the structural changes which accompany Fru-1,6-P_2 activation can, at least partially, compensate for the destabilizing effects of the mutation. These two observations can be explained if thermal inactivation is considered as a rate-limited process. Consequently, either the mutation has destabilized the existing rate-limiting process for thermal inactivation or has altered the rate-limiting process in the mutant enzyme. This explanation is consistent with another mutation in BSLDH (Thr-198→Val) which affects only the Fru-1,6-P_2-activated form of the mutant (Nicholls et al., 1993).

The mutation Asn-143 had a large effect on the GdmCl-equilibrium unfolding profile, which was estimated to destabilize the folded conformation by about 22 kJ/mol (Figure 5). With respect to stabilization energy hydrogen-bonding interactions involving the charged side-chain of Asp-143 would be stronger than a similar interaction with an uncharged residue (Asn-143). This is due to the greater dipole induced in the charged hydrogen bond by the large polarizing effect of the electronegative carboxylic acid group. This type of ionic interaction would be strengthened by the low dielectric environment of Asp-143, which is screened from the solvent by the hydrophobic side-chains of residues in α1F, βK, βL and α2F. Substituting Asp-143 by Asn would weaken the charged hydrogen-bonding interaction by removing the ionic component. In addition the potential for a double hydrogen-bonding interaction is lost with Asn-143, because although the carbonyl group of the Asn-143 side-chain can act as a proton acceptor for hydrogen bonding the amine group cannot. The extent of hydrogen bonding in the mutant enzyme is unknown, therefore GdmCl unfolding shows that the charged hydrogen-bonding interaction of Asp-143 contributes at least 22 kJ/mol to the conformational stability of the BSLDH apoenzyme. This value agrees closely with the minimum estimate for the energy of a charged hydrogen-bonding interaction between tyrosyl-tRNA synthetase and its substrate of at least 17 kJ/mol (Fersht et al., 1985).

Conclusion

It is apparent that the effects elaborated by the mutant enzyme are centred around a structural weakness induced by Asn-143 which results in loss of 22 kJ/mol conformational folding energy in the tertiary structure. Structural evidence suggests that in the wild-type enzyme the Asp-143 side-chain carboxylate group is important for linking three discontinuous elements of the secondary structure, α1F, βK and the β-turn βG-βH. A double hydrogen-bonding interaction is formed where the side-chain carboxylate group of Asp-143 acts as a hydrogen-bond acceptor

for protons donated by both the side-chain hydroxyl group of Ser-273 and the main-chain amide group of His-195. Substitution of Asp-143 by Asn would be expected to destabilize these hydrogen-bonding interactions in two ways: (i) both oxygen atoms of the Asp-143 side-chain carboxylate group are potential proton acceptors; however, only the carbonyl group of the Asn-143 side-chain is a potential proton acceptor thus removing one of the hydrogen-bonding interactions, or (ii) a charged hydrogen-bonding interaction is stronger than an uncharged interaction (Fersht et al., 1985), this effect would be enhanced in the hydrophobic environment of residue Asp-143, which is extensively screened from the solvent by α1F, βK, βL and α2F. The electrostatic calculations predict an increase of pyruvate K_m, and support an increase in non-productive binding of pyruvate, as was found experimentally. In contrast, the results for His-195 pK_a were apparently opposite to those found by experiment.

As Asp-143 appears to be conserved primarily for a structural reason in LDHs it is not immediately obvious why this residue is conserved as Asn-143 in the structurally analogous enzyme MDH. Modified Stern–Volmer plots suggested that the difference in $(K_Q)_{eff.}$ between the wild-type and mutant enzymes was due to charge repulsion between Asp-143 and iodide ions. As oxaloacetate is more negatively charged than the preferred LDH substrate, pyruvate, a similar mechanism suggests that the negative carboxylate side-chain of Asp-143 could decrease the bimolecular rate constant (k_3) for collision of oxaloacetate in a favourable orientation with enzyme·NADH to form a productive ternary complex. In this respect it is significant that the side-chain carboxylate group of Asp-143 is comparatively closer (about 9 Å) to the substrate-binding site than the fluorophores, Trp-80, Trp-150 and Trp-203, which are over 2.8 nm (28 Å), 1.2 nm (12 Å) and 1.8 nm (18 Å) from the carboxylate group of Asp-143 respectively. The reason for different amino acid conservation in LDH and MDH at position 143 may therefore be related to substrate specificity by excluding catalytically competent complexes of oxaloacetate in the substrate-binding site due to charge repulsion in the wild-type LDH enzyme. However, any subtle changes in the relative oxaloacetate specificity of the mutant enzyme Asn-143 will have been masked by the large detrimental effects of the mutation on enzyme structure and the generalized effects of this on catalysis. A parallel analysis of Asn-143 in MDH is currently under investigation.

Received 21 July 1993/2 December 1993; accepted 9 December 1993

We would like to thank Dr. A. R. Clarke for his help with the preparation of this manuscript and Mr. K. Fantom for oligonucleotide synthesis. This work was supported by a grant from the Department of Trade and Industry. Thanks also to the S.E.R.C. M.R. Initiative for computing support.

REFERENCES

Barstow, D. A., Clarke, A. R., Chia, W. N., Wigley, D., Sharman, A. F., Holbrook, J. J., Atkinson, T. and Minton, N. P. (1986) Gene **46**, 47–56

Birktoft, J. J. and Banaszak, L. J. (1984) Pept. Protein Rev. **4**, 1–46

Birktoft, J. J., Fernley, R. T., Bradshaw, R. A. and Banaszak, L. J. (1982) Proc. Natl. Acad. Sci. U.S.A. **79**, 6166–6170

Clarke, A. R., Atkinson, T., Campbell, J. W. and Holbrook, J. J. (1985) Biochim. Biophys. Acta **829**, 387–396

Clarke, A. R., Evington, J. R. N., Dunn, C. R., Atkinson, T. and Holbrook, J. J. (1986) Biochim. Biophys. Acta **870**, 112–126

Dixon, M. and Webb, E. C. (1979) in Enzymes (Dixon, M. and Webb, E. C., ed.), 3rd edn., pp. 138–164, Academic Press, New York

Dauber-Osguthorpe, P., Roberts, V. A., Osguthorpe, D. J., Wolff, J., Genest, M. G. and Hagler, A. T. (1988) Proteins **4**, 37–47

Fersht, A. R., Jian-Ping, S., Knill-Jones, J., Lowe, D. M., Wilkinson, A. J., Blow, D. M., Brick, P., Carter, P., Waye, M. M. Y. and Winter, G. (1985) Nature (London) **314**, 235–238

Gelpi, J. L., Jackson, R. M. and Holbrook, J. J. (1993) J. Chem. Soc. Farad. Trans. **89**, 2707–2716

Gilson, M. K., Sharp, K. A. and Honig, B. H. (1987) J. Comp. Chem. **9**, 327–335

Hart, K. W., Clarke, A. R., Wigley, D. B., Waldman, A. D. B., Chia, W. N., Barstow, D. A., Atkinson, T., Jones, J. B. and Holbrook, J. J. (1987) Biochim. Biophys. Acta **914**, 294–298

Holbrook, J. J. and Stinson, R. A. (1973) Biochem. J. **131**, 739–748

Lehrer, S. S. (1971) Biochemistry **10**, 3254–3263

Nicholls, D. J., Wood, I. S., Nobbs, T. J., Clarke, A. R., Holbrook, J. J., Atkinson, T. and Scawen, M. D. (1993) Eur. J. Biochem. **212**, 447–455

Pace, C. N., Shirley, B. A. and Thompson, J. A. (1989) in Protein Structure (Creighton, T. E., ed.), pp. 311–330, IRL Press, Oxford

Piontek, K., Chakrabarti, P., Schar, H.-P., Rossman, M. G. and Zuber, H. (1990) Proteins **7**, 74–92

Sambrook, T., Fritsch, E. F. and Maniatis, T. (1989) Molecular Cloning: A Laboratory Manual, Cold Spring Harbor Laboratory Press, Cold Spring Harbor, N.Y.

Smith, C. J., Clarke, A. R., Chia, W. N., Irons, L. I., Atkinson, T. and Holbrook, J. J. (1991) Biochemistry **30**, 1028–1036

Waldman, A. D. B., Hart, K. W., Clarke, A. R., Wigley, D. B., Barstow, D. A., Atkinson, T., Chia, W. N. and Holbrook, J. J. (1988) Biochem. Biophys. Res. Commun. **150**, 752–759

Wigley, D. B., Gamblin, S. J., Turkenburg, J. P., Dodson, E. J., Piontek, K., Muirhead, H. and Holbrook, J. J. (1992) J. Mol. Biol. **223**, 317–335

Wilkinson, A. J., Fersht, A. R., Blow, D. M. and Winter, G. (1983) Biochemistry **22**, 3581–3586

Winter, G., Fersht, A. R., Wilkinson, A. J., Zoller, M. and Smith, M. (1982) Nature (London) **299**, 756–758